Available online at www.sciencedirect.com

ScienceDirect

Procedia Computer Science 90 (2016) 113 – 118

Procedia Computer Science

International Conference On Medical Imaging Understanding and Analysis 2016, MIUA 2016, 6-8 July 2016, Loughborough, UK

Luminance Adaptive Biomarker Detection in Digital Pathology Images

Jingxin Liu[a], Guoping Qiu[a,*], Linlin Shen[b]

[a]*The University of Nottingham Ningbo China, 199 Taikang East Road, Ningbo, 315100, China*
[b]*ShenZhen University, Nanhai Ave 3688, Shenzhen, 518060, China*

Abstract

Digital pathology is set to revolutionise traditional approaches diagnosing and researching diseases. To realise the full potential of digital pathology, accurate and robust computer techniques for automatically detecting biomarkers play an important role. Traditional methods transform the colour histopathology images into a gray scale image and apply a single threshold to separate positively stained tissues from the background. In this paper, we show that the colour distribution of the positive immunohistochemical stains varies with the level of luminance and that a single threshold will be impossible to separate positively stained tissues from other tissues, regardless how the colour pixels are transformed. Based on this, we propose two novel luminance adaptive biomarker detection methods. We present experimental results to show that the luminance adaptive approach significantly improves biomarker detection accuracy and that random forest based techniques have the best performances.

Peer-review under responsibility of the Organizing Committee of MIUA 2016

Keywords: Immunohistochemistry, diaminobenzidine, image analysis, luminance, Random Forest;

1. Introduction

Diaminobenzidine (DAB) is one of the most commonly used stains in Immunohistochemistry (IHC), which gives a brown colouration (positive) against a blue background (negative) counter-stained by Hematoxylin. Measuring the positively stained areas can provide qualitative assessments of the tissues[1,2]. Traditionally, this is done manually which is not only labour intensive but also prone to subjective errors. With the increased usage of IHC, it calls for Computer Aided Diagnosis (CAD) systems to support pathologists' decision making. Specifically, we need to develop automatic methods for separating the positively stained tissues from other tissues.

In the literature, various computer-assisted approaches have been developed to separate DAB stained tissues in digital histopathology images[3,4,5,6,7,8,9,10,11,12,13]. Although significant progresses have been made in separation accuracy, there are still several factors affecting the performances of those automatic approaches. For example, visual inspection of Fig.1 (left side) will find that there are a variety of different shades of positively stained (brown colours) tissues

* Corresponding author. Tel.: +44 115 951 4251 Fax.: +44 115 9514254.
E-mail address: guoping.qiu@nottingham.edu.cn

Peer-review under responsibility of the Organizing Committee of MIUA 2016
doi:10.1016/j.procs.2016.07.032

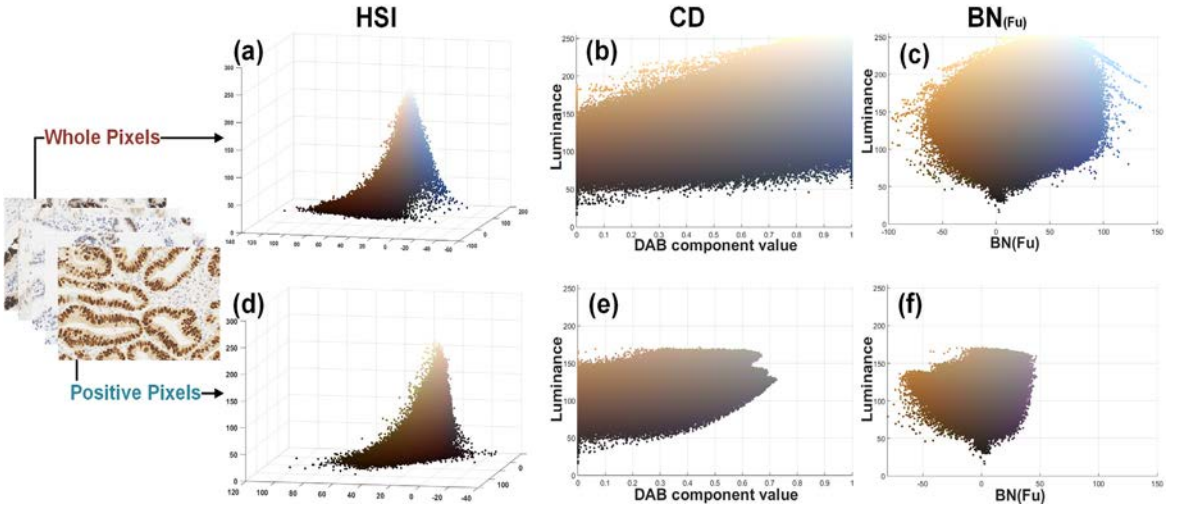

Fig. 1: Visualizations of pixels of P53 stained histopathology images in the colour spaces of three previous methods. Top row: all pixels. Bottom row: Manually labelled positive pixels.

caused by different concentrations of the chemicals, different thicknesses of the tissue slides, and sensor differences amongst many other factors. Accurately identifying these variety of brown colours poses significant challenges to computer algorithms.

In contrast to existing methods that mostly employ simple classification techniques, we firstly propose a Luminance Adaptive Multiple Thresholding (LAMT) method to improve the traditional single thresholding based approaches. Secondly, we develop an advanced machine learning technique termed Luminance Adaptive Random Forest (LARF) classification method for DAB stain segmentation and quantification. Based on the nature of the problem, our model is an ensemble of random forests, each sub-forest works independently and is adapted to a specific level of luminance. We will present experimental results to show that Luminance Adaptive approaches can significantly improve the separation performance, and random forest is ideally suited for biomarker detection.

2. Related Works

Researchers have proposed to convert the original RGB images into other colour spaces to eliminate the correlation in RGB model[13]. The Hue image from the HSI model has been used alone[4], while Goto[5] and Kohlberger[6] classified DAB stained pixels by thresholding all three channels. Pham[3] adapted Yellow channel in CMYK model, which is believed to have strong correlation with the DAB stain. These simple thresholding based classification schemes are straightforward and easy to implement. However, the overlap of different stains in the colour spectrum will make it very difficult to separate the stains completely thus hindering the accuracy of stain detection[13].

Colour deconvolution (CD) is perhaps one of the most well known stain separation approaches first presented by Ruifrok and Johnston[8] in 2001. CD was developed based on the properties of light passing through material according to Beer-Lambert law. Ruifrok proposed to deconvolve the RGB image into three stain component images. The positive stained tissues are separated by thresholding the DAB component image. However, DAB does not follow the Beer-Lambert law as the DAB reaction product has a broad and featureless spectrum[14].

Approaches based on mathematical transformation of RGB images are also popular. The G/B image was used for DAB selection[10], while Ruifrok[11] presented the brown image calculated from RGB image. Two different Blue Normalization (BN) filters[12,13] were proposed. These methods separate DAB stain by thresholding transformed single channel images. However, those methods cannot accurately select the positive stained tissues due to broad colour spectrum of DAB.

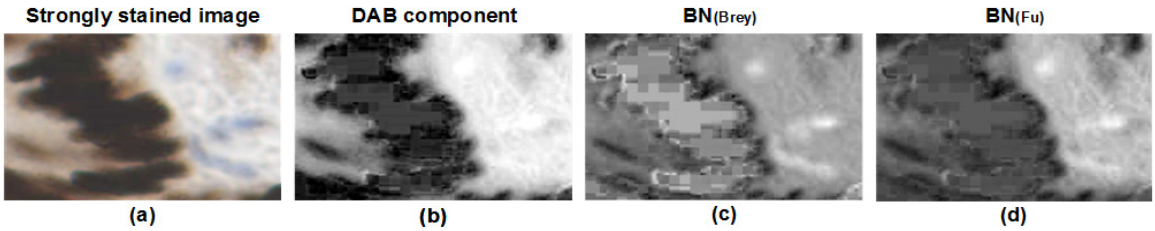

Fig. 2: The comparison of resulted single channel images of strong stained tissues using three previous works. (a) the original digital image of strongly stained tissues; (b) the DAB channel from decovoluted image using CD [8]; (c) and (d) transformed single channel images using BN_{Brey} [12] and BN_{Fu} [13] respectively.

Fig.1 plots the pixels of Hematoxylin-diaminobenzidine (H-DAB) images in the colour spaces of three typical previous methods mentioned above. Fig.1(a) and (d) respectively illustrate the pixels in the HSI cylindrical space for all pixels and manually labelled positive DAB stain only. The pixel distributions taper as the intensity increases. At low intensity, the DAB stain has a significantly broader hue spectrum. Similar plots for the other two colour spaces are respectively shown in Fig.1(b), (c), (e), and (f). Previous approaches to DAB biomarker detection in digital histopathology images are based on transforming the original colour channels to form a single channel in which thresholding is applied to separate the biomarker from the background. Fig.2 illustrates an example of the resulted single channel image of a heavily stained tissues using three previous methods mentioned before. It is seen that using simple thresholding cannot completely separate the stains especially if the stained tissues are dark.

3. Luminance Adaptive Approach for DAB Stain Detection

We treat luminance as one of the most important information in this work. Pixels are divided into specific luminance intervals before thresholding or classification. Luminance represents the luminous intensity of images, and human vision has finer spatial sensitivity to luminance. Different from luma, luminance is the weighted sum of RGB components without gamma-correction. In this paper, normalized luminance $l(\mathbf{p})$ for each pixel is calculated according to the ITU-R BT.709:

$$l(\mathbf{p}) = (0.2126 \cdot R + 0.7152 \cdot G + 0.0722 \cdot B)/255. \tag{1}$$

3.1. Luminance Adaptive Multiple Thresholding

To improve the performance of single threshold approaches, we use multiple thresholds $T = \{t_1, t_2, ..., t_I\}$ on the final single channel images. Specifically, the transformed pixel $\tau(\mathbf{p})$ using traditional methods is divided into I equal intervals according to the luminance:

$$\tau_i(\mathbf{p}) = \{\tau_i(\mathbf{p}) \in \tau(\mathbf{p}) | \xi_i < l(\mathbf{p}) \leq \zeta_i\}, i = 1, ..., I \tag{2}$$

where ξ_i, ζ_i are lower and upper boundary of ith luminance interval. Then we threshold the transformed pixel with different values according to its luminance instead of a single threshold. Thus, the threshold t_i is assigned using binary classification as follows:

$$t_i = \underset{c \in \mathcal{Y}}{\operatorname{argmax}}\, P(c|\tau_i(\mathbf{p})) \tag{3}$$

where $\mathcal{Y} = \{c_0, c_1\}$ is the label.

3.2. Luminance Adaptive Random Forest

In this work, we treat DAB stain separation, DAB biomarker detection as a pattern recognition problem and employ one of the most successful classification models, random forest, at its core. Considering the stain's spectrum spread varies with intensities, we explicitly adapt the random forests to different luminance levels. We believe this is the first time a powerful pattern recognition technique has been applied to the detection of biomarkers in digital histopathology images.

3.2.1. Feature Extraction

For each pixel $\mathbf{p}$, we extract three different types of features to form a 5 dimensional feature: $\mathbf{v}(\mathbf{p}) = (\mathbf{v}_{DAB}, \mathbf{v}_{Cr}, \mathbf{v}_{Cb}, \mathbf{v}_H, \mathbf{v}_S) \in \mathbb{R}^5$. $\mathbf{v}_{DAB}$ is the DAB component of CD image calculated according to pre-set stain vectors[8].We propose to convert the RGB images into YCbCr colour space, and extract Cb and Cr channel information. YCbCr is a method of encoding RGB information, rather than an absolute colour space. Cb and Cr are chroma components of blue-difference and red-difference respectively, which is similar to the BN filter mentioned above. The properties of YCbCr are very suitable for DAB separation. The main ingredient of DAB stained brown colouration is *Red*, followed by *Green* and *Blue*; while hematoxylin-stained tissues are *Blue*. Therefore, two different stains can be accurately separated according Cb and Cr information. In this study, YCbCr values are converted from normalized RGB data based on ITU-R BT.709. In addition, Hue and Saturation channel values of HSI model are also involved, since the components are correlated better with human perception of color.

3.2.2. Forest Training and Test

Similar to LAMT, the training process firstly divides the extracted feature $\mathcal{X}$ into I equal intervals according to the luminance:

$$\mathcal{X}_i = \{\mathbf{v}(\mathbf{p}) \in \mathcal{X} | \xi_i < l(\mathbf{p}) \leq \zeta_i\}, i = 1, ..., I \tag{4}$$

In our method, instead of training a single forest, our model is an ensemble of I sub-forests: $\mathbf{\Psi} = \{\mathbf{\Psi}_1, \mathbf{\Psi}_2, ..., \mathbf{\Psi}_I\}$. The size of each forest is K, while the whole system has $N = K \times I$ trees. The sub-forest $\mathbf{\Psi}_i$ is trained independently with corresponding training set $\mathcal{X}_i$.

The linear split function is used for node splitting, which is setting a threshold on one feature dimension of $\mathbf{v}(\mathbf{p})$. For binary classification, the best situation is that the subset on child nodes are pure containing only positive or negative stained pixels. In this case, we use the widely utilized information gain criterion[15]:

$$Score = \triangle E = -\frac{|\mathcal{S}_l|}{|\mathcal{S}|} E(\mathcal{S}_l) - \frac{|\mathcal{S}_r|}{|\mathcal{S}|} E(\mathcal{S}_r) \tag{5}$$

where $\mathcal{S}$ is the training set at split point, while $\mathcal{S}_l$ and $\mathcal{S}_r$ represent the training images contained in the left and right child node respectively. $E(\mathcal{S})$ is the Shannon entropy of $\mathcal{S}$, and $|\mathcal{S}|$ is the number of sample contained in $\mathcal{S}$.

Given a new unlabelled pixel $\mathbf{p}^*$, we firstly extract the luminance $l(\mathbf{p}^*)$ and feature $\mathbf{v}(\mathbf{p}^*)$ information. The luminance information will identify which sub-forest this pixel falls into and the features are fed into the sub-forest for decision making. Specifically, $\mathbf{v}(\mathbf{p}^*)$ is pushed through each tree of forest $\Psi_{\widehat{i}}$, if $l(\mathbf{p}^*) \in [\xi_{\widehat{i}}, \zeta_{\widehat{i}}]$.

4. Experimental Results

4.1. Materials

We conducted DAB separation experiments on the digital slides from two different kinds of H-DAB stained images: Whole Slide Images (WSI) and tissue microarray images (TMA). Both are human colorectal adenocarcinomas slides using the biomarker P53 (nuclear activity), and captured with a ×40 objective lens and scanned using a Hamamatsu scanner. Each type contains 50 images of 1680×1050 pixels. The positively stained nuclei pixels were manually labelled as described in[9]. The dataset is available from the authors on request.

4.2. Evaluation Metric

Our results were compared with three state-of-art automated separation approaches: CD[8], Brey's BN[12], and Fu's BN[13]. To verify our luminance adaptive approach, we implemented LAMT on those three previous methods. We compared LARF with two conventional random forest models. One of the models used five dimensional features (5-RF) as described in Section 3.2.1, and the other one was trained with six dimensional features (6-RF), which include the luminance as a feature.

A 2-fold cross validation procedure was employed in the experiment, and we repeated the experiment 10 times to test the robustness of the technique. In each 2-fold cross validation, the images were randomly divided into two parts, one part was used for training and the other for testing.

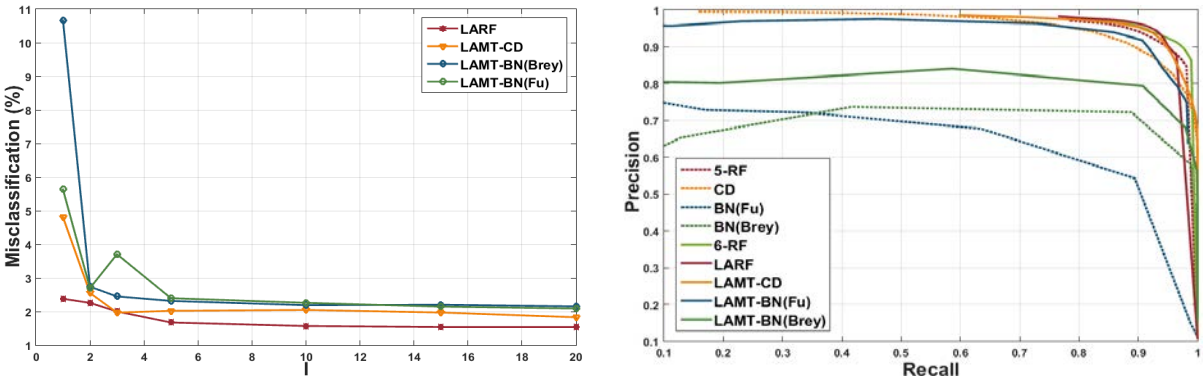

(a) (b)

Fig. 3: (a) The performance comparison with different numbers of luminance interval I. (b) Precision-recall curve of different methods for DAB-stained tissues separation.

The separating results of the proposed method were compared with manual labelled positive stained nuclei tissues. We employed two criteria to measure the accuracy: misclassification and F1 score.

$$MisClassification = \frac{\sum \text{Misclassified area}}{\text{Total image area}}; \tag{6}$$

F1 score is the harmonic mean of precision and recall, where precision and recall are defined as $P = \frac{|TP|}{|TP|+|FP|}$ and $R = \frac{|TP|}{|TP|+|FN|}$ respectively.

4.3. Results

We firstly performed experiments to test the performance of each method for different numbers of luminance intervals I. Fig.3(a) shows that the misclassification rates decrease significantly as I increases for all four methods. We found that $I = 10$ worked well and further increase I did not improve the results. It is seen that our method achieves the lowest misclassification rate across all I followed by LAMT-CD. Fig.3(b) shows the precision-recall curves for each approaches, again, our technique performed the best. Table 1 summarises a comparison of misclassification performances (averaged over 10 experiments) of traditional single threshold and LAMT ($I = 20$) on three previous techniques; while Table 2 compares the results of random forest based approaches. It is seen that using the Luminance Adaptive approach, all methods have seen a significant improvement.

Table 1: Performance comparison of traditional single thresholding method and LAMT method with three previous approaches.

Method	Misclassification (%)	F1 Score	Method	Misclassification (%)	F1 Score
CD [8]	4.81	0.812	LAMT – CD	1.83	0.884
BN_{Brey} [12]	10.66	0.714	LAMT – BN_{Brey}	2.15	0.877
BN_{Fu} [13]	5.63	0.780	LAMT – BN_{Fu}	2.09	0.831

Table 2: Misclassification and F1 score of random forest based methods.

Method	Misclassification (%)	F1 Score
5-RF	2.38	0.863
LARF	**1.53**	**0.905**
6-RF	1.89	0.887

It is also worth noting that a random forest that included the luminance as a feature (6-RF) also achieved a lower misclassification rate (1.89%) than all previous methods. This demonstrates that random forest can be used as a powerful classifier for accurately detecting biomarkers in digital pathology images. In this case, the luminance is treated by the random forest as a separate feature and the ways it is used for separating the biomarkers are found through

the random forest construction mechanism. Whilst including luminance as a feature worked well, pre-segmenting the luminance and building sub-forests adaptive to the luminance level gave the best performances.

Consequently, the result indicates that hitherto ignored luminance is the key for solving the problem of incomplete separation caused by DAB featureless colour spectrum, and packet-based DAB stained pixel selection according its luminance is simple and efficient.

5. Conclusion

In this paper, we have presented a novel quantitative analysis tool for H-DAB stained digital images. Our model treats luminance as a very important information for DAB segmentation, and trains several sub-forests separately each adapted for a specific level of luminance. We conducted a series of experiments to evaluate the new method. The results demonstrate that misclassification errors can be significantly reduced by including luminance information in the decision making for both traditional methods and for random forest classifier. Luminance adaptive random forest approach is shown to give the best performances.

Acknowledgements

This work is partially supported by Ningbo Science and Technology Bureau (Project No 2012B10055 and 2013D10 008), the Natural Science Foundation of China (61272050), Natural Science Foundation of Guangdong Province (2014A030313556) and the International Doctoral Innovation Centre (IDIC) at the University of Nottingham Ningbo China.

References

1. Varghese, F., Bukhari, A.B., Malhotra, R., De, A.. Ihc profiler: an open source plugin for the quantitative evaluation and automated scoring of immunohistochemistry images of human tissue samples. *PloS one* 2014;**9**(5):e96801.
2. Rakha, E., Soria, D., Green, A.R., Lemetre, C., Powe, D.G., Nolan, C.C., et al. Nottingham prognostic index plus (npi+): a modern clinical decision making tool in breast cancer. *British journal of cancer* 2014;**110**(7):1688–1697.
3. Pham, N.A., Morrison, A., Schwock, J., Aviel-Ronen, S., Iakovlev, V., Tsao, M.S., et al. Quantitative image analysis of immunohistochemical stains using a cmyk color model. *Diagnostic pathology* 2007;**2**(1):8.
4. Ma, W., Lozanoff, S.. A full color system for quantitative assessment of histochemical and immunohistochemical staining patterns. *Biotechnic & histochemistry* 1999;**74**(1):1–9.
5. Goto, M., Nagatomo, Y., Hasui, K., Yamanaka, H., Murashima, S., Sato, E.. Chromaticity analysis of immunostained tumor specimens. *Pathology-Research and Practice* 1992;**188**(4):433–437.
6. Kohlberger, P., Breitenecker, F., Kaider, A., Lösch, A., Gitsch, G., Breitenecker, G., et al. Modified true-color computer-assisted image analysis versus subjective scoring of estrogen receptor expression in breast cancer: a comparison. *Anticancer research* 1998;**19**(3B):2189–2193.
7. Ruifrok, A.C., Katz, R.L., Johnston, D.A.. Comparison of quantification of histochemical staining by hue-saturation-intensity (hsi) transformation and color-deconvolution. *Applied Immunohistochemistry & Molecular Morphology* 2003;**11**(1):85–91.
8. Ruifrok, A.C., Johnston, D.A.. Quantification of histochemical staining by color deconvolution. *Analytical and quantitative cytology and histology/the International Academy of Cytology [and] American Society of Cytology* 2001;**23**(4):291–299.
9. Shu, J., Qiu, G., Ilyas, M., Kaye, P.. Biomarker detection in whole slide imaging based on statistical color models. In: *MICCAI 2010 Workshop on Computational Imaging Biomarkers for Tumors: From Qualitative to Quantitative*. 2010, .
10. Montironi, R., Diamanti, L., Thompson, D., Bartels, H., Bartels, P.. Analysis of the capillary architecture in the precursors of prostate cancer: recent findings and new concepts. *European urology* 1995;**30**(2):191–200.
11. Ruifrok, A.C.. Quantification of immunohistochemical staining by color translation and automated thresholding. *Analytical and quantitative cytology and histology/the International Academy of Cytology [and] American Society of Cytology* 1997;**19**(2):107–113.
12. Brey, E.M., Lalani, Z., Johnston, C., Wong, M., McIntire, L.V., Duke, P.J., et al. Automated selection of dab-labeled tissue for immunohistochemical quantification. *Journal of Histochemistry & Cytochemistry* 2003;**51**(5):575–584.
13. Fu, R., Ma, X., Bian, Z., Ma, J.. Digital separation of diaminobenzidine-stained tissues via an automatic color-filtering for immunohistochemical quantification. *Biomedical optics express* 2015;**6**(2):544–558.
14. van der Loos, C.M.. Multiple immunoenzyme staining: methods and visualizations for the observation with spectral imaging. *Journal of Histochemistry & Cytochemistry* 2008;**56**(4):313–328.
15. Fu, H., Zhang, Q., Qiu, G.. Random forest for image annotation. In: *Computer Vision–ECCV 2012*. Springer; 2012, p. 86–99.